cnme 2016
10º Congresso Nacional de Mecânica Experimental

EXPERIMENTS ON EARTH DAMS BREACHING. MONITORING INSTRUMENTATION AND METHODS

Sílvia Amaral
Departamento de Hidráulica e Ambiente, Laboratório Nacional de Engenharia Civil

Teresa Viseu
Departamento de Hidráulica e Ambiente, Laboratório Nacional de Engenharia Civil

Ana Margarida Bento
Secção de Hidráulica, Rec. Hídricos e Ambiente, Faculdade de Engenharia da Universidade Porto

Ricardo Jónatas
Departamento de Hidráulica e Ambiente, Laboratório Nacional de Engenharia Civil

Laura Caldeira
Departamento de Geotecnia, Laboratório Nacional de Engenharia Civil

Rafaela Cardoso
CERIS, Instituto Superior Técnico, Universidade de Lisboa

Rui M. L. Ferreira
CERIS, Instituto Superior Técnico, Universidade de Lisboa

RESUMO

A research project on laboratorial characterization of the breach processes involved in the failure by overtopping of earth dams is currently ongoing at LNEC and IST. The breach evolution process is a complex phenomenon which requires the understanding of both hydraulic and geotechnical components involved. Laboratorial tests allowed relating the dynamics of the breach with the hydraulic and geotechnical properties of the embankments and understanding how the latter influence the failure mechanisms. In this paper four different approaches for estimating breach hydrographs are presented. Two are based on: i) stage-discharge relations; and ii) water-volume balances within the reservoir. The other two constitute a novel estimating method and are both based on velocity field maps, obtained from the application of an LSPIV algorithm and on breach area detection, delineated with the aid of a laser sheet. The technique used for combining the instrumentation and measuring methods in these different approaches for breach hydrographs estimation is herein scrutinized.

Keywords: Earth dam / Overtopping / Breach hydrograph / LSPIV algorithm / Breach area

1. INTRODUCTION

Failures of earth dams have distinct reasons, being piping the main cause of failure, followed by overtopping, with 46% and 36% of failures, respectively around the world between 1940 and 2000 (Foster *et al.* 2000). Different failure mechanisms may be observed depending on the type of dam and construction soil (Singh 1996). For cohesive soils, the breach forms through headcuts that deepen and enlarge over time (Hanson *et al.* 2005), whereas the failure process through non-cohesive soils tends to develop through progressive surface erosion (Visser 1998; Coleman *et al.* 2002). The discharge hydrograph of the breaching dam (herein called breach hydrograph) can thus greatly differ depending on the main characteristics of the dam. This corresponds to the major source of uncertainty in risk assessment studies.

The main objective of this research is to quantify the breach hydrograph following the overtopping of earth dams. To accomplish this objective, a 0.45 m high scaled earth dam was subjected to overtopping under well controlled laboratory conditions. Breach hydrograph estimates from experimental data have been obtained by several different methods that can be divided in two different types: i) indirect estimates - obtained with data collected far from the dam; ii) direct estimates - obtained with data collected at the dam site. A novel direct method, based on LSPIV and on breach area detection, is presented and its quality is assessed by comparison with the results obtained by those using indirect estimates more commonly used.

Among the indirect estimates, those based on stage-discharge relations (rating curves) and on water-volume balances within the reservoirs are the most commons. Stage-discharge relations are fitted from a set of simultaneous stage and discharge measurements at a control section downstream the breaching dam (Rantz *et al.* 1982). The accuracy of these estimates is undermined if the control section is not close enough to the breaching dam, so that inertial effects cannot be negligible and the discharge may not be representative of the breach hydrograph. Estimates obtained with water volume balances within the reservoir are usually computed from the reservoir elevation and storage records (Singh 1996; Morris *et al.* 2007).

Direct estimates have been based on mechanical velocimeters (Muste *et al.* 2008) that produce velocity distributions to be integrated in the cross-section. The application of these mechanical devices is, in general, time consuming as the velocity points are sampled one by one. On the other hand, dam-breach flows, even at a laboratorial scale, are still highly transient and therefore easily disturbed by intrusive devices. Hence, the application of this

method in highly unsteady flows is strongly inadvisable. Acoustic Doppler Velocimeters (ADV) have also been employed on transient flows measurements. Nonetheless, in dam-breach flows these velocimeters have the following drawbacks: i) do not provide continuous observations; ii) require the use of seeding; and iii) are intrusive devices (Bastiaans 2000; Yorke and Oberg 2002; Tauro *et al.* 2014). Remote methods such as radar (Costa *et al.* 2006) and image-based (Fujita *et al.* 1998; Harpold *et al.* 2006) velocity measurements have been used as non-intrusive equipment's in a wide range of flow conditions. As one of the remote image-based techniques, the Large Scale Particle Image Velocimetry (LSPIV) has gained increasing popularity in surface velocity measurements for offering superior efficiency, performance and reliance than the traditional mechanical instrumentation (Muste *et al.* 2008). It consists in recording the movement of seeded fluid and estimating the particles displacement from pairs of consecutive images through cross-correlation techniques (Adrian 1991; Raffel *et al.* 2007).

2. DAM-BREACH EXPERIMENT

2.1 Experimental facility

The experiment was conducted in a medium scale laboratory channel, 31.5 m long and 6.60 m wide, at LNEC, Portugal. Fig. 1 illustrates the general view of the channel and the experimental setup.

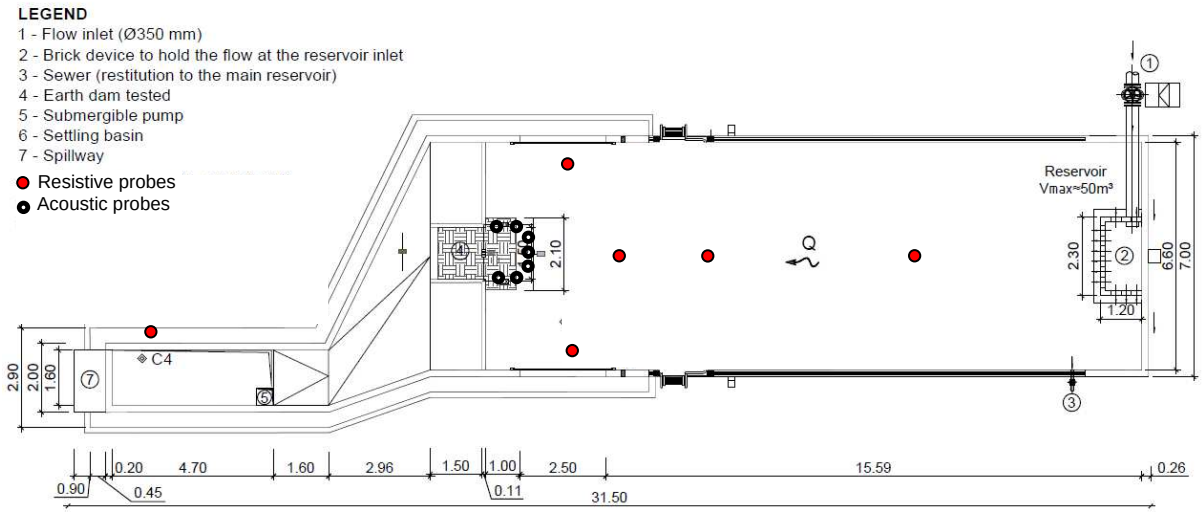

Fig. 1 – Plan view of the experimental facility (dimensions in meters)

The scaled model, a 0.45 m high earth dam composed by a silty sand material (soil fractions: 7% gravel, 66% sand and 27% non-plastic fines), was conducted to overtopping. The sediments from the dam failure were collected in a settling basin (length=4.4m; width=1.7m

and depth=0.60m - 6 in Fig. 1) equipped with a rectangular spillway (7 in Fig. 1) located at the channel downstream end.

More details about earth dam dimensions, soil properties and compaction procedures can be found in Bento (2013) and Jónatas (2013).

2.2 Instrumentation and experimental procedures

Several variables were measured during the dam-breach experiment (Fig. 2): (i) the flow discharge at the reservoir inlet; (ii) the water level in the reservoir and in the settling basin; (iii) the surface flow velocity field near the breach; (iv) the breach geometry evolution; and (v) the free-surface elevation in the vicinity of the breach. Measurements (i) and (ii) were used to obtain an indirect estimate of the breach hydrograph based on the reservoir's mass balance. Measurements (ii) were used to obtain an indirect estimate based on the rating curve of the downstream spillway. Measurements (iii), (iv) and (v) allowed for the direct estimates of the breach hydrograph.

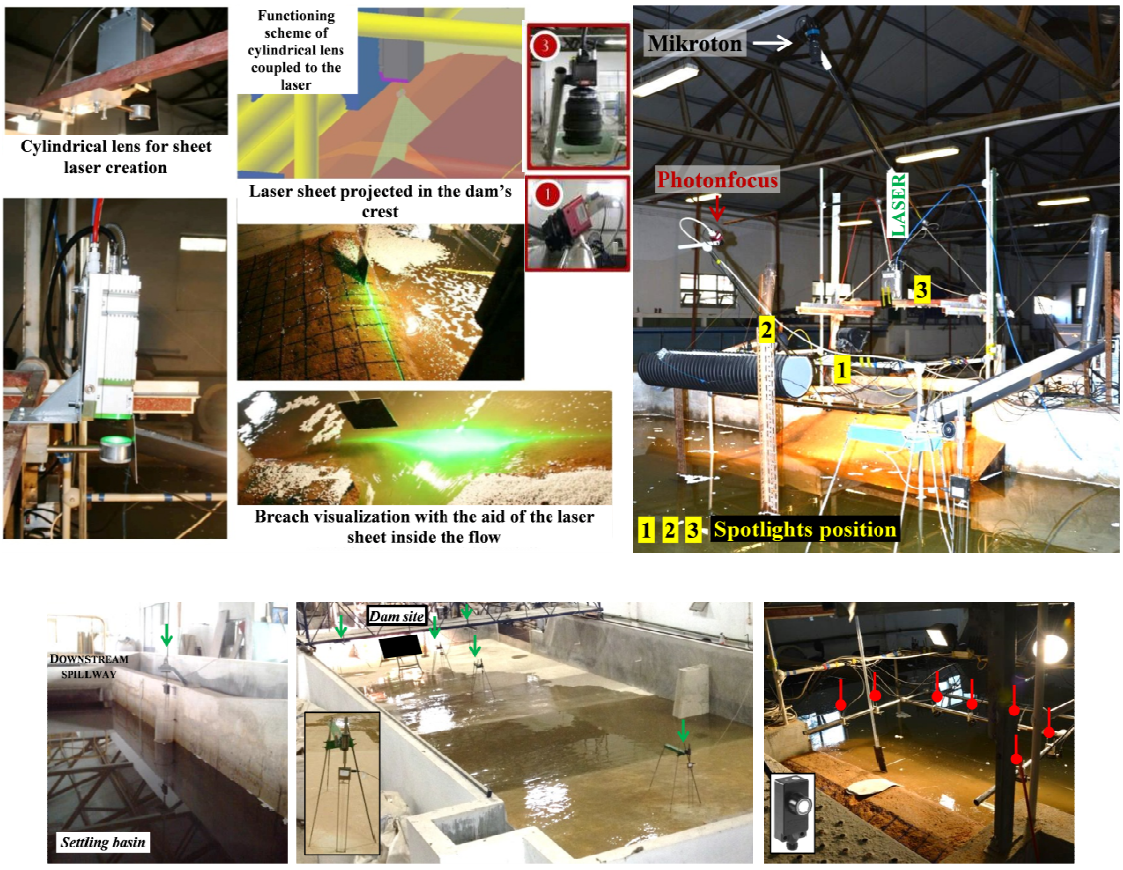

Fig. 2 – Instrumentation implemented in the experimental facility

The inflow discharge, controlled by a manual valve at the channel entrance, was real-time recorded by a digital flowmeter. The water levels in the reservoir and in the settling basin were measured by limnimeters and resistive probes. Two limnimeters were placed at the channel lateral walls while three resistive probes were distributed within the reservoir. A resistive probe was placed inside an acrylic cylinder in the settling basin to avoid signal acquisition disturbances caused by free-surface oscillations.

Regarding surface velocity measurements, instantaneous maps were obtained with the open-source PIVlab software (Thielicke and Stamhuis 2014) applied to the overhead images obtained with a high-speed video camera (MotionScope M3). Styrofoam beads with a mean diameter of 3 mm and a density of 1.05 gcm^{-3} were used as tracer particles.

The breach geometry evolution and the free-surface position in the vicinity of the breach during the experiment were determined by digital image post-processing. Both were delineated with a vertical laser sheet created by a cylindrical lens from a 1 mm radius continuum green laser beam (532 nm). A second high-speed video camera (PhotonFocus) was placed upstream aligned with the dam crest center, registering the intersection of the laser sheet with the media interfaces, namely the free-surface and the breach geometry under water. An additional digital camera (Sony DCR-SX 53E), positioned downstream the dam, was used to record the profile of the breach formation and erosion evolution of the downstream face of the dam during the overtopping.

A frame rate of 150 fps was adopted in MotionScope M3 to avoid in-plane loss of pairs (Hart 2000) during the application of LSPIV algorithms for the computation of velocity maps near the dam-breach. A proper illumination, provided by 2 spotlights combined with a reduction on the camera light exposure, enabled good image contrast and the catching of small displacements of the seeding particles upon the shutter opening. A small camera light exposure time was adopted in PhotonFocus to avoid image blurring.

The definition of the breach initiation instant (t=0s) was prompted by the sudden removal of a metallic plate when the upstream level reached the crest level allowing the flow through the pilot channel at the crest centerline. The image acquisition with all the cameras (HD and high speed) and the signal acquisition from resistive probes, limnimeters and discharge meters was initiated at the breach initiation instant (t=0s).

Further details regarding the experimental procedure, the instrumentation and the respective acquisition software can be found in Bento (2013).

2.3 Data processing

Images from the MotionScope M3 and PhotonFocus high-speed digital video cameras were processed to determine the surface velocity maps and the breach geometry, respectively, envisaging a direct calculation of the breach hydrograph. The signal from resistive probes, limnimeters and flowmeter, necessary for the indirect estimates, were subjected to basic signal filtering including despiking and denoising.

The surface velocity maps were obtained from the evaluation of image pairs separated by a small finite time step (in this case, Δt=1/150s). The images sequence obtained with the MotionScope M3 camera were used for this purpose, being previously subjected to imaging pre-processing techniques to increase its quality and therefore the results accuracy (Raffel *et al.* 2007). A threshold high-pass filter with a cut-off of 150px was chosen, to emphases tracer contrast against the background and to eliminate noise due to inhomogeneous lightning (Thielicke 2014).

The evaluation of image pairs was performed with a cross-correlation method (Pust 2000). The cross-correlation function for two discretely sampled images is defined by the following expression, which statistically measures the match degree between a pair of images, deriving the most probable particle displacement in each interrogation area:

$$\Phi_{f_g}(m,n) = \sum_i^M \sum_j^N f(i,j)g(i+m,j+n) \quad (1)$$

with f(i,j) and g(i,j) denoting the image intensity distribution of the interrogation areas of the first and second image at (i,j) location, respectively, m and n the pixel offset between the two interrogation areas, M and N, the number of rows and columns, respectively $\Phi_{f_g}(m,n)$ and the cross-correlation function (see variables in Fig. 3).

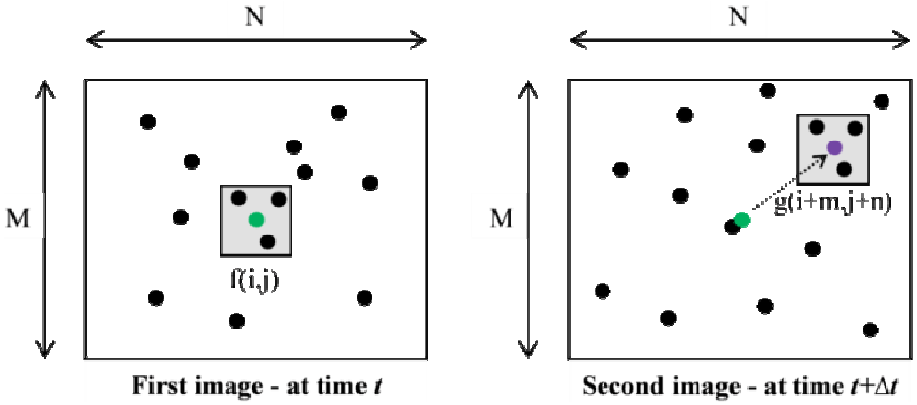

Fig. 3 – Pair of PIV images frames

Equation (1) was solved by a discrete Fourier transform (DFT) approach (Keane and Adrian 1992; Raffel *et al.* 2007), both available in PIVlab software (Thielicke and Stamhuis 2014).

Velocity maps in know units are obtained through image calibration. Two horizontal rulers fixed to an aluminum bar suspended over the flow by two floating blocks were used in this experiment as measuring units (Fig. 4). These followed the water surface decrease during the test contemplating the distance variations between the camera and the water surface. The floating blocks were far enough so that the flow field and the erosion process would not be affected.

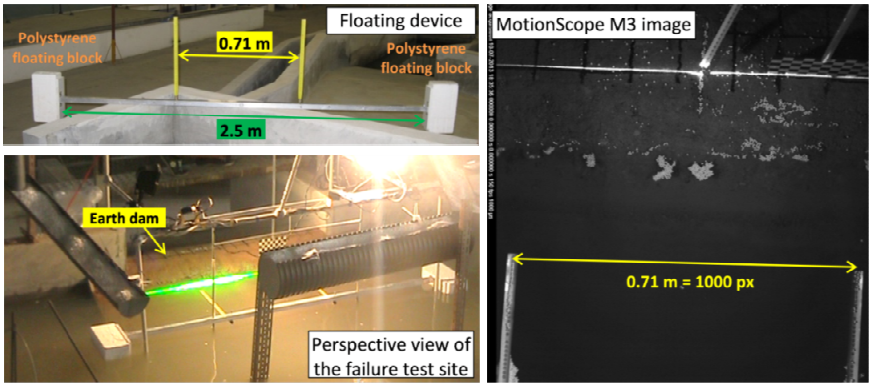

Fig. 4 – Calibration of the MotionScope M3 images. Horizontal rulers coupled to floating blocks

The breach area was determined through analysis of the images acquired with the PhotonFocus and MotionScope M3 high-speed digital video cameras. Two different approaches were followed to define the breach shape (Fig. 5):

Approach A - the intersection of the submerged dam body with the laser sheet; The breach bottom corresponds to the bright line resulting from the intersection of the laser sheet with the submerged dam body (the trace of the dam body) - a technique used in a different context by Soares-Frazão *et al.* (2007);

Approach B - the crest line formed between the undisturbed upstream dam slope and the breach channel; The crest line corresponds to the bright line resulting from the intersection of the laser sheet with the air-water interface. This crest line is detected as a brighter region, shaped as an arc, in the images of the MotionScope M3 camera.

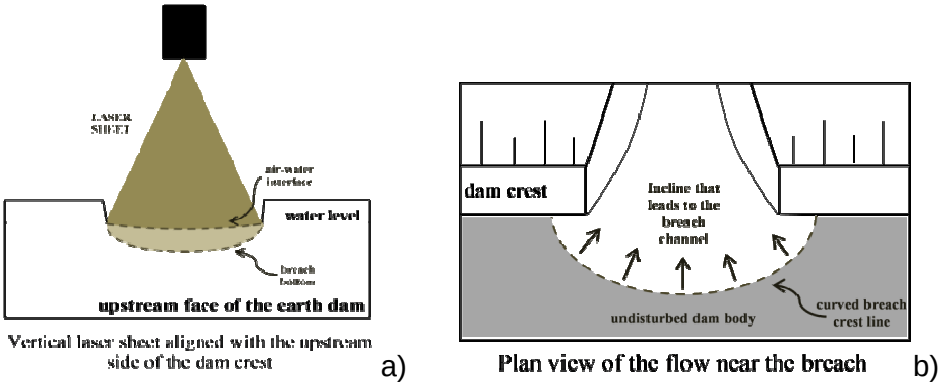

Fig. 5 –Breach area definitions: a) approach A (perspective image); b) approach B (plain image)

A chess plate of know dimensions was aligned with the laser sheet and partially submerged in the reservoir to be included in the images captured with the PhotonFocus camera for calibration purpose. The submerged part of the plate allowed for the determination of the experimental refraction index (i_{exp} = 1.45). This value is close to the theoretic index of (i_{theor} = 1.33), being the difference attributed to water turbidity (Reyes-Coronado *et al.* 2005).

Determining the free-surface elevation of unsteady flows requires signal post-processing to eliminate noise and spurious values (Leal *et al.* 2006; Soares-Frazão *et al.* 2012). In this work, the free-surface elevation inside reservoir was determined by three resistive probes, two limnimeters and seven acoustic probes placed in the breach vicinity (Fig. 1). A resistive probe was also placed at the channels downstream settling basin for this purpose. The probes and discharge meter signals were first despiked with a simple threshold criterion applied to detrended data (trend was subsequently added back). A common zero was then determined during a time interval of constant free-surface elevation taken before the initiation of the test and the same elevation was assigned to all probes in this time interval. Then the signal was filtered to eliminate electric noise but also small amplitude surface waves. For this purpose, the power spectral density function of the signal corresponding to the constant free-surface time interval was analysed. It was found that surface waves were associated to frequencies of 0.5-2 Hz. Hence, small frequencies were attenuated with a low pass first-order digital Butterworth filter with a cut-off frequency of 0.5 Hz.

3. RESULTS

3.1. Direct estimates of the breach hydrograph

The direct estimates of the breach hydrograph were obtained as the product of flow velocities and breach areas (see Eq. (2)):

$$Q = \int_A u_s \,.\, n dS \approx U_n A \tag{2}$$

Where u_s is the surface velocity at the breach section, n is the unit normal vector pointing out of the reservoir, A is the breach flow area and U_n is the depth-averaged flow velocity normal to the breach section.

As previously mentioned in section 2, two different approaches were followed to determine the breach area: (A), based on the intersection of the laser sheet with the submerged dam body and with the free-surface and (B), where the breach area is that of the fluid region above the crest line.

A comparison between the two direct estimates is plotted in Fig. 6 a). For lower discharges, the two estimates denote the same increase tendency. As the breaching process develops, the rate of increase of estimate (A) becomes markedly smaller than that of estimate (B), a trend that, as denoted in next section 3.2, is not supported by the indirect estimates. This may be due to the limitations introduced by the width of the laser sheet: the normal velocity in estimate (A), which coincides with the streamwise velocity in channel coordinates, should be integrated over the entire channel planar cross-section. For small breaches, this is not a major drawback since the longitudinal velocities are small everywhere except in the vicinity of the breach. For larger breaches, the longitudinal velocity beyond the illuminated region becomes increasingly important and failing to considering it introduces no negligible errors.

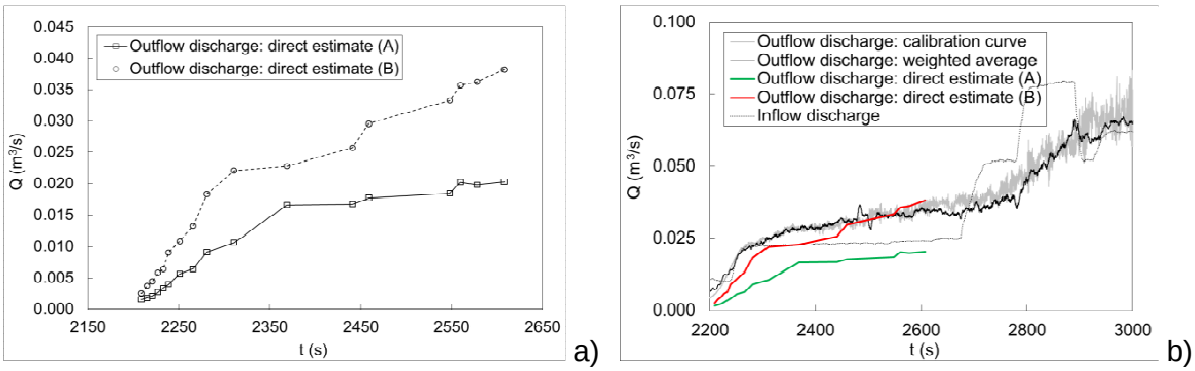

Fig. 6 – Breach hydrograph: a) Direct estimates; b) Comparison of the direct estimates of the breach hydrograph with the mass balance estimate and the downstream rating curve

3.2. Indirect estimates and comparison with the direct estimates of the breach hydrograph

Two indirect methods to estimate the breach hydrograph were considered. The first used the rating curve of the spillway installed in the settling basin while the second was obtained by applying the mass balance equation in the reservoir. The rating curve of the spillway was empirically determined in the laboratory on the basis of water level above the crest and discharge pairs (H, Qs): different flow discharges were imposed at the inlet and the resistive probe placed in the settling basin, measured the correspondent flow depths over the spillway crest. A polynomial function was then applied to fit the filtered measured data. The mass balance equation in the reservoir consisted of an explicit forward differencing scheme of the reservoir's continuity. Detailed descriptions are provided in Bento (2013) and Jónatas (2013).

Fig. 6 b) shows the breach hydrographs obtained from the two indirect estimates and the two direct estimates. Time evolution of the inflow discharge is also shown for completeness. Generally, direct and indirect estimates reveal a good overall agreement. However, it is

noted that the discharge estimate based on the mass balance in the reservoir is prone to spurious oscillations since it is a quantity obtained from numerical differentiation thus likely to amplify small perturbations in the primitive signal.

The direct estimate obtained through approach (A) is in general agreement with both the mass balance and rating curve hydrograph estimates: the rates of increase are similar and the values are similar. Particularly encouraging is the response of the direct estimate to the break in the inflow hydrograph that occurs approximately at $t = 2250$ s. Both indirect estimates, mass balance and rating curve, respond almost immediately, registering a decrease in their positive slope. The direct hydrographs estimates should follow this trend since these are based on the data collected at the breach vicinity, from where it would be expected that, at the breach entrance, the discharge would also respond almost immediately. In this particular aspect, as the same type of response was observed, this is taken as highly encouraging.

4. CONCLUSIONS

Dam breaching following overtopping invariably faces morphological changes of both hydraulic and geotechnical nature. It is believed that the link between hydraulic and geotechnical phenomena is a necessary step towards a better understanding and definition of dam breach hydrographs. Thus, in the present work, two indirect and two direct breach hydrograph estimates were undertaken under well-controlled laboratory conditions.

The novel and direct methods herein introduced appear to be promising alternatives for modeling dam-breach overtopping failures. They require expensive instrumentation with complex calibration processes and, at this stage, are still limited to the study of small breaches. However, they served as a proof of concept proved to be robust and non-intrusive methods with potential to become powerful tools to evaluate and discuss the impact of sudden mass detachments during overtopping failure and consequent inertial effects.

The breach hydrograph estimates discussed in this paper resulted from accurate data gathered with recent and suitable instrumentation and measuring methods. The instrumentation and measuring methods adopted in these experiments were chosen among several others which were also tested and either did not serve the purpose or not reached the desired accuracy degree. Therefore, the final instrumentation set-up endorsed the achievement of accurate data, allowing the discussion of the applicability extent of each breach hydrograph estimates herein presented.

5. REFERENCES

Adrian, R. J. 1991. Particle-imaging techniques for experimental fluid mechanics, Annu. Rev. Fluid Mech., 23(1), p. 261–304.

Bastiaans, R. 2000. Cross-correlation PIV; theory, implementation and accuracy, Eindhoven University of Technology, Faculty of Mechanical Engineering, Eindhoven.

Bento, A. M. 2013. Characterization of dam breaching following overtopping, MSc. Thesis, Instituto Superior Técnico, Universidade de Lisboa.

Coleman, S. E., Andrews, D. P., and Webby, M. G. 2002. Overtopping breaching of noncohesive homogeneous embankments, Journal of Hydraulic Engineering, 128(9), p. 829–838.

Costa, J. E., Cheng, R. T., Haeni, F. P., Melcher, N., Spicer, K. R., Hayes, E., Plant, W., Hayes, K., Teague and Barrick, D. 2006, Use of radars to monitor stream discharge by noncontact methods, Water Resour. Res., 42(7).

Foster, M., Fell, R., and Spannagle, M. 2000, The statistics of embankment dam failures and accidents, Canadian Geotechnical Journal, 37(5), p. 1000–1024.

Fujita, I., Muste, M., and Kruger, A. 1998, Large-scale particle image velocimetry for flow analysis in hydraulic engineering applications. Journal of Hydraulic Research, 36(3), p. 397–414.

Hanson, G., Cook, K., and Hunt, S. 2005. Physical modeling of overtopping erosion and breach formation of cohesive embankments, Transactions of the ASAE, 48(5), p. 1783–1794.

Harpold, A. A., Mostaghimi, S., Vlachos, P. P., Brannan, K., and Dillaha, T. 2006, Stream discharge measurement using a large-scale particle image velocimetry (LSPIV) prototype,Transactions of the ASABE, 49(6), p. 1791–1805.

Jónatas, R. 2013. Rotura de barragens de aterro por galgamento. Ensaios experimentais com aterros homogéneos, MSc. Thesis, Faculdade de Ciências, Universidade de Lisboa.

Keane, R. and Adrian, R. 1992. Theory of cross-correlation analysis of piv images, Applied Scientific Research, 49(3), p. 191–215.

Leal, J., Silva, P., and Ferreira, R. 2006. Dam-break propagation over a movable bed in a non-prismatic channel, River Flow 2006, Taylor & Francis (aug).

Morris, M., Hassan, M., and Vaskinn, K. 2007. Breach formation: Field test and laboratory experiments, Journal of Hydraulic Research, 45(sup1), p. 9–17.

Muste, M., Kim,W., and Fulford, J. M. 2008. Developments in hydrometric technology: new and emerging instruments for mapping river hydrodynamics, Bulletin - The journal of the World Meteorological Organization.

Pust, O. 2000. Piv: Direct cross-correlation compared with fft-based cross-correlation, Proceedings of the 10th International Symposium on Applications of Laser Techniques to Fluid Mechanics, Lisbon, Portugal, Vol. 27, p. 114.

Raffel, M., Willert, C., and Kompenhans, J. 2007. Particle Image Velocimetry: a practical guide, Springer, Berlin Heidelberg.

Rantz, S. E. (1982). Measurement and computation of streamflow: Volume 1, Measurement of stage and discharge. USGPO

Reyes-Coronado, A., García-Valenzuela, A., Sa´nchez-Pérez, C., and Barrera, R. G. 2005. Measurement of the effective refractive index of a turbid colloidal suspension using light refraction. New J. Phys., 7.

Singh, V. P. 1996. Dam Breach Modeling Technology. Springer Netherlands.

Soares-Frazão, S., Grelle, N. L., Spinewine, B., and Zech, Y. 2007. Dam-break induced morphological changes in a channel with uniform sediments: measurements by a laser-sheet imaging technique, Journal of Hydraulic Research, 45(sup1), p. 87–95.

Soares-Frazão, S., Canelas, R., Cao, Z., Cea, L., Chaudhry, H. M., Moran, A. D., Kadi, K. E., Ferreira, R., Cadórniga, I. F., Gonzalez-Ramirez, N., Greco, M., Huang, W., Imran, J., Coz, J. L., Marsooli, R., Paquier, A., Pender, G., Pontillo, M., Puertas, J., Spinewine, B., Swartenbroekx, C., Tsubaki, R., Villaret, C., Wu, W., Yue, Z., and Zech, Y. 2012. Dam-break flows over mobile

beds: experiments and benchmark tests for numerical models, Journal of Hydraulic Research, 50(4), p. 364–375.

Tauro, F., Olivieri, G., Petroselli, A., Porfiri,M., and Grimaldi, S. 2014. Technical note: Surface water velocity observations from a camera: a case study on the tiber river, Hydrology and Earth System Sciences Discussions, 11(10), p. 11883–11904.

Thielicke, W. (2014). The Flapping Flight of Birds - Analysis and Application. PhD Thesis. University of Groningen.

Thielicke, W. and Stamhuis, E. J. 2014. PIVlab – towards user-friendly, affordable and accurate digital particle image velocimetry in MATLAB, Journal of Open Research Software, 2.

Visser, P. 1998. Breach growth in sand-dikes, Hydraulic and Geotechnical Engineering Division, Faculty of Civil Engineering and Geosciences, Delft University of Technology, Delft.

Yorke, T. H. and Oberg, K. A. 2002. Measuring river velocity and discharge with acoustic doppler profilers, Flow Measurement and Instrumentation, 13(5-6), p. 191–195.

ACKNOWLEDGMENTS

The authors thank the team of the Laboratory of Construction and Modeling, the Geotechnical Department and the Centre of Scientific Instrumentation of the National Laboratory of Civil Engineering (LNEC) for the technical assistance in all the experimental work. This work was partially funded by FEDER, program COMPETE, and by national funds through Portuguese Foundation for Science and Technology (FCT) project RECI/ECM-HID/0371/2012. The first author also thanks FCT for financial support through PhD scholarship SFRH/BD/47694/2008.